Smart Agricultural Technology 11 (2025) 100907

Contents lists available at ScienceDirect

Smart Agricultural Technology

journal homepage: www.journals.elsevier.com/smart-agricultural-technology

Design of a low-cost gas accumulation chamber for general purpose environmental monitoring

Domenico Longo [a], Serena Guarrera [a], Delia Ventura [a], Emanuele Cerruto [a,*], Salvatore Roberto Maugeri [b], Gaetano Giudice [b]

[a] Department of Agriculture, Food and Environment of University of Catania (Di3A-UniCT), Via S. Sofia 100, 95123 Catania, Italy

[b] Istituto Nazionale di Geofisica e Vulcanologia, Sezione di Catania, Osservatorio Etneo (INGV-OE), Piazza Roma 2, 95125 Catania, Italy

ARTICLE INFO

Keywords:
Soil/Water CO_2 flux
Low-cost CO_2 flux measurement
Agriculture
Volcanology
Environment

ABSTRACT

The need for accurate measurement of CO_2 emissions from surfaces arises from various fields, particularly in precision agriculture, irrigation water management, wastewater management, volcanology, geothermal exploration, environmental and climate monitoring. This study introduces a novel, cost-effective closed dynamic accumulation chamber system designed to measure CO_2 fluxes from soil and water surfaces. A short review of existing measurements techniques is provided, alongside a detailed explanation of key algorithms used for processing field data. The proposed system collects raw CO_2 concentration data via an internal data logger. A custom-developed software suite enables real-time first-approximation flux calculation through a user-friendly Javascript web application compatible with smartphones with any type of operating system and web browser. A freely available Matlab® tool allows for post-processing data analysis for a more accurate flux calculation. After calibration against the commercial PP Systems EGM-5, assumed as a reference, some case studies in agriculture, wastewater treatment and volcanic environments demonstrate the instrument's versatility, showcasing its potential for advance in agricultural field and environmental sustainability.

1. Introduction

Since the 1960s [1], greenhouse gas (GHG) fluxes to the atmosphere from various anthropogenic activities and natural sources, such as volcanoes, mud volcanoes, mofettes, peatlands and wetlands, have gained relevance in various fields of human society and scientific contexts. This pertains to understanding the impact of human activities or natural events on climate change and, more broadly, to the artificial modification of the global environment. These fluxes are constantly monitored by various local institutions. In addition, organizations such as the World Meteorological Organization [2], Smithsonian Environmental Research Center [3] and the Deep Carbon Observatory [4], in recent decades have funded research studies, among many others, on natural emissions from the Earth's deep interior (core, mantle, crust).

Among GHGs, CO_2 plays a major environmental role due to its abundance and greenhouse effect. The proposed instrument and its field applications focus on this gas, primarily in the context of volcanology, as well as in agronomic and wastewater treatment plants.

Regarding volcanic monitoring, emissions of CO_2 and other significant gases have been measured in peripheral and summit areas of active volcanoes [5,6] and in geothermal areas [7–13]. CO_2 emission monitoring can help to understand the evolution of volcanic activity in different scenarios [6]. Volcanoes emit significant amounts of gases into the atmosphere not only during volcanic unrests but also during periods of quiescence. Variations in the emission rate of CO_2, correlated with other geochemical signals, have been observed before eruptive periods [14,7,15,16] and are also associated with strong earthquakes [17]. In volcanic environments, CO_2 emissions have been noted during seismic swarms without consequent volcanic activity [9]. Among the magmatic gases released by volcanoes, CO_2 is the second most abundant after H_2O [18]. In recent years, the availability of CO_2 sensors, particularly non-dispersive infrared (NDIR) spectrometers, which are sufficiently robust and reliable, has enabled diffuse degassing studies worldwide, as well as continuous monitoring with permanent stations using different methods [19–23]. Currently, variations in the CO_2/H_2O ratio and in total degassing rate of CO_2, are considered potential indicators of

All authors have read and agreed to the published version of the manuscript.

* Corresponding author.
E-mail address: emanuele.cerruto@unict.it (E. Cerruto).

https://doi.org/10.1016/j.atech.2025.100907
Received 25 November 2024; Received in revised form 21 March 2025; Accepted 23 March 2025
Available online 24 March 2025

renewal magmatic fluid activity, suggesting imminent unrest or significant changes in volcanic activity [18].

Regarding the agronomical field, it must be noted that soils represent a major global carbon stock, sensitive to climate change and ecosystem feedback [24–26]. In this context, monitoring soil gas fluxes is important to assess CO_2 concentration (in both soil and atmosphere) and its exchange through the soil-atmosphere interface under different agriculture scenarios [27]. Climate change is the primary limiting factor in the development of sustainable agricultural production. Generally, atmospheric CO_2 positively affects agroecosystems by increasing crop photosynthesis, water use efficiency, and fruit growth [28]. On a global scale, annual CO_2 emissions from agronomical soils are approximately 10 times greater than those from fossil fuel combustion, but they are naturally counterbalanced by a similar flux in the opposite direction through plant activity [24,29,30].

Soil CO_2 and agronomical processes are closely linked due to strong interactions between soil, plant roots exudates, soil fungi and bacteria, but understanding them is complex due to the simultaneous interaction of many different sub-ecosystems. Indeed, this link dominates both base rates and short-term fluctuations in soil CO_2. In this sense, the different components of soil CO_2 have been suggested as indicators of ecosystem metabolism. Many methods are available to measure these gas fluxes and their main components [31]. In agricultural systems, agronomic management practices can influence soil CO_2 in several aspects, such as nitrogen-rich fertilizations, which increase soil CO_2 activity [32]. Therefore, monitoring CO_2 fluxes is fundamental to evaluate the impact on soil CO_2 with a view to sustainable and conservative agriculture.

In the wastewater management field, significant sources of CO_2 emissions are due to organic compound degradation. Wastewater treatment plants accelerate these conversions, assuming a significant role in GHG emissions [33], from 3 % to 4 % globally [34]. However, the contribution of the wastewater sector to CO_2 emissions may be underestimated [35]. Nowadays, treatment wetlands (TWs) are applied as resilient, low cost and extensive decentralized eco-technologies able to cope with the main challenges related to wastewater management, like natural water quality impairment and water scarcity [36]. Different studies assess the carbon footprint of conventional and natural wastewater treatment plants (e.g., [37–39]), emphasizing their contribution to global GHG emissions, but with not clear differences. In fact, existing studies often rely on estimates based on literature emission rates [40] and underline the importance of incorporating real GHG emissions measured on-site in full-scale wastewater treatment plants for more accurate assessments [41,42]. CO_2 emissions in TWs are limitedly reported, with values significantly depending on the type of TWs and wastewater treated, suggesting that TWs achieve significant carbon sequestration similar to natural wetlands. Also, several factors influence CO_2 emissions from TWs, including hydraulics, environmental conditions, seasonal changes, and plants physiology [43], such as root exudates and rhizosphere processes [44]. Therefore, the efficient monitoring of CO_2 emissions in TWs system can be advantageous for both their optimized management and promotion as a strategic nature-based solution for wastewater treatment and reuse.

Different methods and techniques have been developed over time to measure these gaseous exchanges, depending on the particular context [45,46]. Particularly in soil/atmosphere and water/atmosphere interactions, the most common method to compute fluxes is the accumulation chamber [47,21,23]. This technique uses a known volume connected to the soil or water surface through an open surface, initially air-filled with atmospheric gas concentration, allowing measurement of the variation of gas concentration inside the volume, caused by the flux under measurement. This basic working principle, where the unknown soil/water gas flux to the atmosphere is proportional to the rate of variation of gas concentration inside the chamber, has been improved over time. Many devices, manual or automatic, are described in scientific articles and prototype presentations (e.g., [48,8,49,5,50]), and many are commercially available.

Several approaches have been developed: dynamic, static, open and closed methods, with or without CO_2 scrubbing systems (soda lime) [19,20,45]. Various technical solutions have been proposed to address ground coupling with different types of soil [27], internal chamber pressure compensation [51], in order to minimize errors due to instrument interference with the flux under measurement. Furthermore, different methods to automatically reset the gas composition inside the chamber to atmospheric background levels at the beginning of the measurement have been developed; this allows for long-term, automatic, non-supervised monitoring. In particular, the most common solution is a mechanical moving lid with electric actuators [52–55].

In this work, the development of a compact, opaque, closed-volume dynamic accumulation chamber device for CO_2 flux measurement with a purging system that does not use mechanical moving parts, able to reset the measuring volume to the initial atmospheric condition, is presented. This design makes the proposed system relatively inexpensive compared to other commercial systems and less prone to faults. While commercial systems are suitable for research use, their high cost is prohibitive for example for farms wishing to implement Precision Agriculture techniques using multiple chambers. Additionally, the simplified mechanical design makes the system more robust and reliable. It can be installed in the field for several days or years and allows measurements on saturated soil or, when equipped with a floater, on the water surface [56]. It is also possible to easily replace the chamber volume with others having different heights, as it is simply screwed to the instrument body using a gasket.

To ensure a proper soil seal, limit adverse wind effects and underground lateral leaks, a collar with holes buried in the soil can be used. The chamber is made of non-transparent PVC, as photosynthetic activity inside the chamber is not considered. The chamber is equipped with its own sensor suite, dedicated electronics for manual or automatic CO_2 flux measurements and a smartphone-enabled WiFi user interface. The developed system was compared to a reference standard instrument to assess its reliability and was calibrated using state-of-the-art methodology and certified gases. This presentation comprises also a limited selection of case studies that were carried out using the proposed instrument.

2. Material and methods

The present section is divided into several subsections, each devoted to a different aspect of the proposed instrument design. SubSection 2.1 provides a concise comparison of a few commercially available devices. SubSections 2.2, 2.3 and 2.4 describe the developed instrument for the mechanical/pneumatic subsystem, the sensor suite used and the user interface, respectively. SubSection 2.5 explains the algorithm used for flux calculation and the related models. Finally, subSection 2.6 describes the developed tool for data post-processing.

2.1. Comparative analysis of commercial systems

There are different methods for measuring soil CO_2 flux, such as chamber systems, micrometeorological techniques (Eddy Covariance) and soil gas probes [57]. Each method has its advantages and limitations depending on the spatial and temporal scale, accuracy, cost, and ease of use. Chamber systems are devices that usually cover a portion of the soil surface with a known volume and measure the change over time in CO_2 concentration inside the volume, typically using an infrared gas analyzer (IRGA). The CO_2 flux can then be calculated from the rate of that change, the chamber volume and area, barometric pressure, and gas temperature [58–60]. Some of these instruments are manually operated, while others are automatic. The chamber itself can be opaque or transparent, depending on whether internal photosynthetic activity is of interest. These commercial instruments are generally characterized by a very high cost. There are different types of chamber systems:

1. Closed static chambers;
2. Closed dynamic chambers;
3. Open dynamic chambers.

Closed chambers do not allow air exchange with the outside environment; closed dynamic chambers use a pump to circulate air within the volume and the measurement instrumentation. Open dynamic chambers allow air exchange with the outside environment by using a pump with a constant flow rate for air intake. All these instruments can use fans to ensure gas mixing inside the volume.

Closed static chambers are simple and inexpensive, but measurement instrumentation is often inserted inside the chamber and therefore prone to damage. Closed dynamic chambers can avoid these problems, but they can be a bit more complicated and can require more electrical power if they use mechanical moving parts. Open dynamic chambers can minimize disturbance to the soil surface, but they need accurate measurements of intake air flow rate and CO_2 concentration.

Various commercial instruments are available on the market, and Table 1 compares some of them, including the prototype presented in this study, based on common characteristics that may guide the user's choice. Table 1 relies on Author's experience. Most of them use the dynamic closed chamber method; only the ADC Bioscientific ACE can use different working principles and can be configured in different ways. This allows the final user to apply the best method needed based on the specific application. Some of these instruments are portable and suitable for discrete surveys, while others are designed for long-term monitoring. Commonly, the applications of these instruments are in agronomy or forestry. In the fields of volcanological monitoring, some extra protections are needed to guarantee long-term operations with a reasonable level of manual maintenance to withstand harsh environments (chemically aggressive gases, dust, lapilli, etc.). Some of these products also need additional telemetry systems and/or external power supply systems (e.g., batteries, photovoltaic panels, wind generators, etc.).

As can be seen from Table 1, all commercial systems have very high costs. While this may be acceptable for research purposes, where public or private funding is available, or for establishing a reference system, it is often not viable for field applications requiring multiple instruments. The developed system, if assembled in-house, can cost as little as €500. However, when following an engineering process, it can be offered as a commercial system for around €5000 (including real-time and post-processing tools with a graphical user interface), which is less than most other commercial systems. Moreover, since most of the commercial systems use a moving lid to reset the initial chamber gas condition, maintenance issues may arise, requiring operator intervention in the field. This can be hazardous, especially in volcanic environments, where risk levels can be high, making it essential to minimize on-site operator presence.

2.2. Mechanical and pneumatic design of the proposed device

The main structure of the accumulation chamber was made by non-transparent PVC as the photosynthetic activity inside it was not of interest for CO_2 soil flux measurement. It had a cylindrical shape, with a height of 100 mm and a diameter of 200 mm [62–64]. Another similar PVC cylinder, equipped with removable cover, was mounted on top of the chamber to host all the electro-pneumatic sub-systems and sensors (Fig. 1).

The cylindrical shape of the measurement chamber provided a good balance between achieving a better and more uniform distribution of the gas inside the chamber and easy of construction, whereas squared shapes can create non-uniformities in gas distribution. It is also known that chamber height is related to gas saturation behavior inside the chamber, depending on the sampling time duration, gas analyzer full scale capabilities and the expected mean flux level. The height of 100 mm is sufficient for fluxes ranging from few to about 100 g m^{-2} day^{-1}, measured for five or ten minutes [46,64,65]. When greater fluxes are expected, the chamber volume can easily be replaced with others of different heights, as it is simply screwed onto the instrument body using a gasket.

The device was atmospheric pressure-compensated by five small vents of about 2 mm in diameter. One vent was placed between the chamber and the electro-pneumatic sub-systems vane; four vents were placed between this vane and the external atmosphere, designed to limit the Venturi effect caused by wind and so minimizing gas leak from the measurement chamber. The whole assembly is weatherproof when the upper cover is kept closed. To guarantee a soil seal and limit adverse

Table 1
Comparison of various commercial devices, including the prototype presented in this study.

Model	West System Fixed Station	West System Portable Station	Licor 8200	ADC Bioscientific ACE	PP Systems EGM-5 & SRC2	PP System CFLUX-1	Prototype
Reference	West Systems [55]	West Systems [55]	LiCOR, Li-8200 [53]	ADC Bioscientific Ltd, ACE [52]	PP Systems, SBA-5 datasheet [61]	PP Systems, CFlux-1 [54]	This work
Country	Italy	Italy	USA	UK	USA	USA	Italy
Type	closed dynamic chamber	closed dynamic chamber	closed dynamic chamber	can be changed by closing or opening valves	closed dynamic chamber	closed dynamic chamber	closed dynamic chamber
Mixing	fan	fan	measurement pump flux and chamber design	fan and chamber design	fan	measurement pump flux and chamber design	measurement pump flux
Long term	years	days	months	months	days	months / years	years
Automatic monitoring and maintenance	yes, but it needs maintenance for the mechanical parts	only for discrete surveys	yes, but it needs frequent maintenance	yes, but it needs frequent maintenance	only for discrete surveys	yes, but it needs frequent maintenance	yes
Ruggedness	yes	yes	it needs some additional protection	it needs some additional protection	it needs some additional protection	it needs some additional protection	yes
Plug & play for long term monitoring	yes	no	needs to add a power supply and telemetry systems	needs to add a power supply and telemetry systems	no	needs to add a power supply system	needs to add a power supply and telemetry systems
Price in euro (from different Italian resellers, 2024)	50,000	25,000	30,000	12,000	12,000	12,500	500 (in-house assembled) 5000 (from resellers)
Software availability	only purchased	only purchased	only purchased	only purchased	only purchased	only purchased	freely available

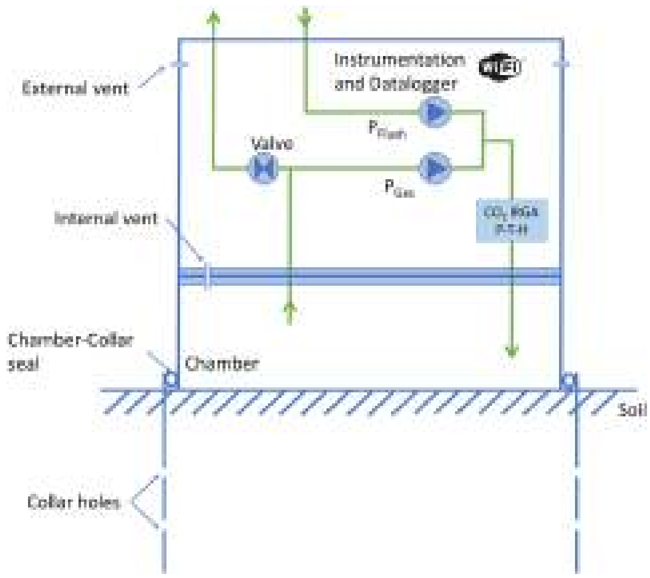

Fig. 1. Schematic diagram of the developed accumulation chamber.

wind effects and underground lateral leaks, a collar buried in the soil can be used. The lower part of the collar featured several holes (about 15 mm in diameter) that allowed gases and roots to enter the collar more easily when it was buried seasonally or year-round [27]. On the other hand, the unperforated upper part of the collar guaranteed a barrier against wind and leaks. The total collar height was 160 mm, which guaranteed mechanical strength and good adhesion to the soil, allowing the chamber to be inserted/extracted in/from the collar through a silicone tight seal without the risk of removing the collar from the terrain. Some soap can be used as lubricant to ease the connection.

A simplified schematic of the pneumatic circuit is shown in Fig. 1. It is composed of two separate parts that share some components. The first part is related to the membrane pump P_{Flush}, which is driven by a 12 V DC brushed motor (Thomas 1410 series). This pump is responsible for the removal of all traces of accumulated gas in the chamber and from all piping. It takes fresh air from the outside through a sintered filter and a PTFE filter (1 μm pore size) at a rate of about 4 L min^{-1}. This flow passes through the IRGA sealed box and then from the chamber back to the atmosphere through the valve (with a 12 V DC solenoid). The choice of the chamber flush pump can be critical, as it may cause soil CO_2 depletion or an incomplete chamber purge. The pump's flow must be chosen based on chamber geometry and subsequently checked to ensure depletion does not occur and that the purge is adequate.

The second part of the circuit is related to the membrane pump P_{Gas}, which is driven by a 12 V DC permanent magnet brushless motor (Thomas 3014 series). Once the valve is closed, this pump takes gas from the chamber at a low rate of about 1 L min^{-1}, passes it through the IRGA, and returns it to the chamber.

The two pipes that take in and release gas inside the chamber have different length to facilitate gas mixing. Additionally, they have two 90° elbow fittings at their ends. This design creates an upwards circular movement of the gas mass inside the chamber, which further aids in gas mixing and prevents gas stratification without the need for a mechanical fan.

Other low-cost prototypes described in the literature differs from the device presented here, mainly for the chamber reset mechanism between two consecutive measurements, while using a very commonly available IRGA sensor.

2.3. Sensors and logging subsystem design

The sensor suite was mainly composed of an IRGA sensor (K-30 by Senseair AB [66]) with a measurement range from 0 to 5000 ppm (some K30 variant can measure in the range from 0 to 10,000 ppm), a measurement error of ± 3 %, and a sample rate of 0.5 Hz. A custom-made data logger (MG2, by [67]) based on the SAM3X Atmel MCU (32-bit ARM Cortex-M3 RISC CPU) was used. The logger has an SD card where configuration parameters and sampled data were stored. Additionally, it has the capability to connect to a remote server using an LTE modem for remote logging, although in the actual configuration the modem is not present.

Since the IRGA is a passive-diffusion type, it was enclosed in a sealed small chamber to measure CO_2 concentration in the flux being measured. A PTH (Pressure-Temperature-Humidity) sensor is enclosed inside the same IRGA chamber to measure the temperature, pressure and humidity of the gas under measurement. However, only pressure and temperature parameters were used in the CO_2 flux calculation. The PTH sensor is a BME280 [68]. The sensor has a temperature error of approximately ± 0.5 °C, a pressure error of approximately ± 100 Pa, and a humidity error of approximately ± 3 %, with a guaranteed sample rate of 1 Hz when acquiring all three parameters.

Every measurement cycle starts with a chamber cleaning phase in which fresh air from the atmosphere is smoothly pumped inside the chamber at about 4 L min^{-1} rate for two minutes to remove previously accumulated CO_2; this can rinse the 3 L chamber volume almost three times, as standard best practice. Exhaust air is discarded back into the atmosphere. At the end of the cleaning phase, a valve seals the chamber with respect to the external atmosphere, and the accumulating gas inside the chamber is pumped into the IRGA at a low rate (about 1 L min^{-1}) and then returned to the chamber. To limit non-linear accumulation rate inside the chamber, the measurement cycle is maintained at 300 s. The working cycle of the system is described in Table 2, along with typical parameter setting and system behavior. The stand-by phase can last indefinitely or be programmed for a defined duration to allow for periodic measurements. In a typical automatic configuration, the stand-by phase is set to last 480 s to achieve a measurement every 900 s. All the different parameters are defined in a configuration file stored on the SD card of the logger.

2.4. User interface

The concentration data set, in ppm, is stored on the onboard data logger and can be accessed in real-time via a WiFi connection. A smartphone (Android or IOS) with any available web browser can be used. The system provides an ad-hoc developed JavaScript web application in which concentration data (along with temperature, pressure, and other parameters) are shown in real-time graphs (Fig. 2). This allows for an initial first-approximation of the measured flux and enables to constant monitoring of the system's behavior and other parameters, such as the state of the battery, the temperature and external pressure

Table 2
System parameters and behavior.

Parameter	Duration	Behavior
Warmup	120 s	WiFi = on P_{Flush} = on P_{Gas} = on Valve = on Sensors = on
Sampling	300 s / 1 Hz	WiFi = on P_{Flush} = off P_{Gas} = on Valve = off Sensors = on
Stand-by	Manual or automatic duration (e.g., 480 s)	WiFi = off P_{Flush} = off P_{Gas} = off Valve = off Sensors = off

Fig. 2. Web application user interface; smartphone screenshot (a) and on a tablet during in-field operation. The upper green circle is a flashing heartbeat indicator for WebSocket connection status.

and the number of measurements made.

Acquired data can also be saved in CSV format on the smartphone. The WiFi interface (Fig. 2) is implemented using an ESP8266 MCU [69]. The MCU receives data from the data logger through its serial port (TTL voltage levels) using a custom ASCII string protocol. The web page and related JavaScript application are stored on the MCU's flash memory and served by a webserver running on the ESP8266. All shown data are asynchronously pumped to the web application through the WebSocket protocol, following the AJAX programming concept.

2.5. Flux calculation algorithm

As reported in literature [58–60], the CO_2 flux from the soil/water surface can be calculated starting from the rate of concentration change inside the chamber volume, the chamber volume and area, barometric pressure and gas temperature. In Fig. 3, a typical measurement dataset is shown; the dead band area and the area of interest for the measurement, with increasing CO_2 concentration values, can be observed.

The flux F is given by [70]:

$$F = S \times K, \text{ expressed in mol m}^{-2}\text{ day}^{-1}, \quad (1)$$

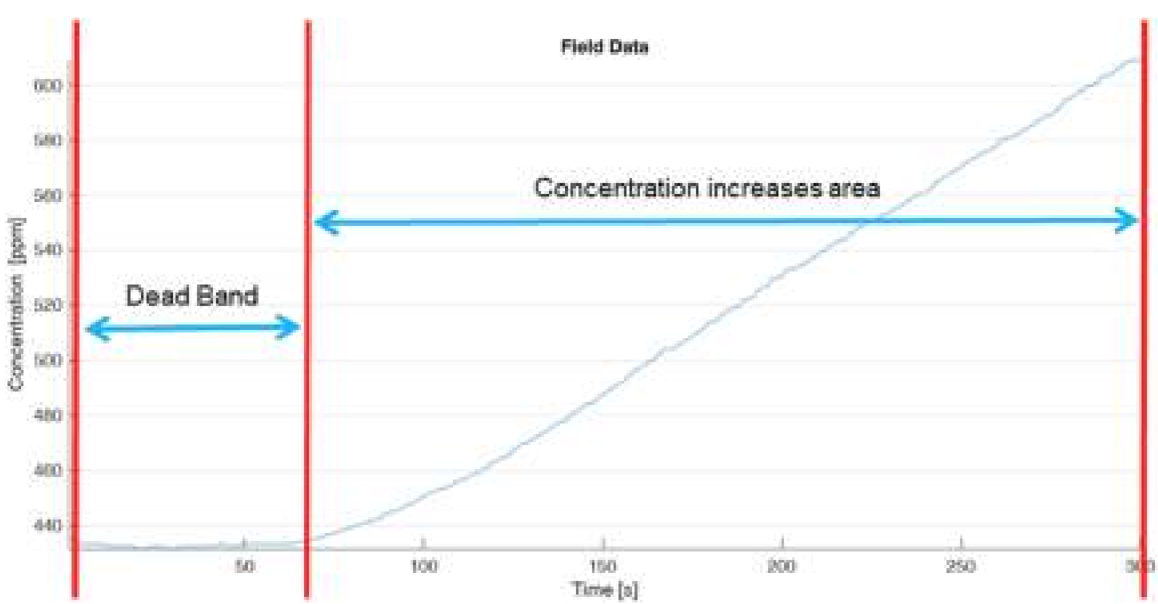

Fig. 3. Highlights of different areas of a typical CO_2 concentration dataset.

where:

S = rate of change in gas concentration within the chamber, expressed in ppm s^{-1}. It corresponds to the slope of the concentration curve computed at the initial point after the dead band; K = accumulation chamber constant, given as reported in Eq. (2):

$$K = \frac{86400}{10^6} \times \frac{p \cdot V}{R \cdot T} \times \frac{1}{A}, \text{ expressed in mol s ppm}^{-1}\text{day}^{-1} \text{ m}^{-2} \tag{2}$$

where:

p is the barometric pressure (Pa);
R is the gas constant 8.3144 (Pa m^3 K^{-1} mol^{-1});
T is the air temperature (K);
V is the chamber volume (m^3);
A is the chamber inlet area (m^2).

The CO_2 concentration time series is usually modelled as a linear Eq. (3), quadratic Eq. (4), or exponential Eq. (5) trend:

$$y = a + bx \tag{3}$$

$$y = a + bx + cx^2 \tag{4}$$

$$y = a + be^{cx} \tag{5}$$

Eq. (5) is the standard model for flux calculation using the accumulation chamber methodology [71,65,72,73]. Eq. (4), utilizing a quadratic model, serves as a second order approximation of the exponential model, derived from the Taylor expansion. Its primary advantage lies in faster computation time, while still yielding results that are only slightly different from those obtained using the exponential model.

If a linear model for the CO_2 concentration time series is used, the slope S is just the slope of the regression line calculated on the data. If quadratic or exponential models are used, the slope to be used is the slope of the line tangent to the model curve, calculated in the initial point, after discarding the dead band (Fig. 3).

2.6. Data processing

A Matlab® tool (MathWorks®, v. 2024b, [74,75]) was developed in order to process CO_2 concentration data time series obtained from the chamber's internal data logger in CSV format. The obtained time series, consisting of 300 samples (sampling time: 1 s), contain CO_2 concentration values inside the chamber over time, along with gas temperature and pressure. These time series typically have a first part with very limited concentration change (dead band, mainly due to internal pneumatic dead volumes) and a second part with an increasing concentration over time (Fig. 3).

The main issue to tackle when dealing with this type of time series, is the detection of the dead band. A possible solution can be based on the RANSAC algorithm (Random sample consensus, [76,77]). This algorithm, usually applied in the computer vision area, is able to estimate target model parameters even when a high number of outliers are present in the data set. Exploiting this feature, it is able to automatically discard the dead band and various other types of noise and outliers in time series data.

In order to calculate CO_2 fluxes, the tool implements different approaches and algorithms:

1. A linear regression (least squares linear regression fit) over the entire dataset Eq. (3);
2. A linear regression (least squares linear regression fit) with a user-selectable subrange (e.g., to manual exclude dead band or other types of measurement noise) Eq. (3);
3. A linear regression (least squares linear regression fit) over the entire dataset, with automatic dead band and noise rejection using the RANSAC algorithm Eq. (3);
4. A three-coefficients least squares quadratic regression fit over the entire dataset, with automatic dead band and noise rejection using the RANSAC algorithm Eq. (4);
5. A three-coefficients least squares exponential regression fit over the entire dataset, with automatic dead band and noise rejection using the RANSAC algorithm Eq. (5).

The algorithm described in point 1 is the simplest and can provide a general idea of the order of magnitude of the flux. However, it is sensitive to outliers and may yield inaccurate results, especially if the dead band is wide.

The algorithm described in point 2 is similar, but it introduces the option to manual set the range of data to be considered in the linear regression. This algorithm is also implemented in the web user interface to provide real-time estimation of the flux. The only difference is that in the web application this algorithm is executed in real-time for each new CO_2 concentration data point.

The algorithm described in point 3 involves a pre-processing phase in which a specifically tuned RANSAC algorithm attempts to exclude the dead band. Subsequently, a least squares linear regression fit is applied on the remaining data. The user is responsible for the final evaluation of the results, and if they are deemed unsatisfactory, it is possible to run another fit. Due to the internal phase of random point selection in the RANSAC algorithm, the final result will typically vary. The algorithms at points 4 and 5 follow the same logic but implement quadratic (Eq. (4)) and exponential (Eq. (5)) regression, respectively.

To assist the user in validating the proposed results, the software computes three statistical parameters for both RANSAC-based regressions, whether linear or quadratic: R^2 (coefficient of determination), RMSE (root mean square error), and the flux 95 % confidence interval. This latter can be calculated in fast mode, using directly the 95 % confidence level of estimated parameters of the linear or quadratic model, or in a more accurate mode, based on a bootstrap method with 400 iterations (by default; user-definable). Subsequently, the software calculates the 2.5 %, 50 % and 97.5 % percentiles of the flux. The median (50th percentile) was used to represent the "true" flux.

All the calculated flux values can be exported in CSV format for further processing. Figs. 4 and 5 illustrate the developed tool processing a concentration dataset. Additionally, the tool is capable of transmitting the entire dataset over a serial port of the PC (RS232, possibly through a USB-to-Serial adapter) for various purposes. For instance, this feature can be utilized for debugging the WiFi user interface.

From a software perspective as well, other prototypes described in the literature differ from the device presented here mainly due to the absence of a graphical user interface and the algorithms used to handle the dead band and the other outliers.

3. Results for system calibration and comparison

The most common commercial instruments similar to the equipment presented in this work [52–55] typically do not report the error in flow measurement. In their respective manuals and technical specifications, only the error introduced by the gas analyzer used to measure the gas concentration in the chamber is reported. However, these kinds of instruments are subjected to various first-order and second-order error sources.

First-order error sources:

- The gas analyzer used has its own measurement error, which represents the main error source. The K30 IRGA has an error of about ± 3 %; the EGM-5 IRGA (PP Systems, SBA-5, 2025) has an error of about ± 1 %.
- The standard gas used for calibration has its own accuracy (about ± 2 %, as per the used gas cited below).
- The mathematical model used (linear or exponential) present uncertainty in parameters estimation.

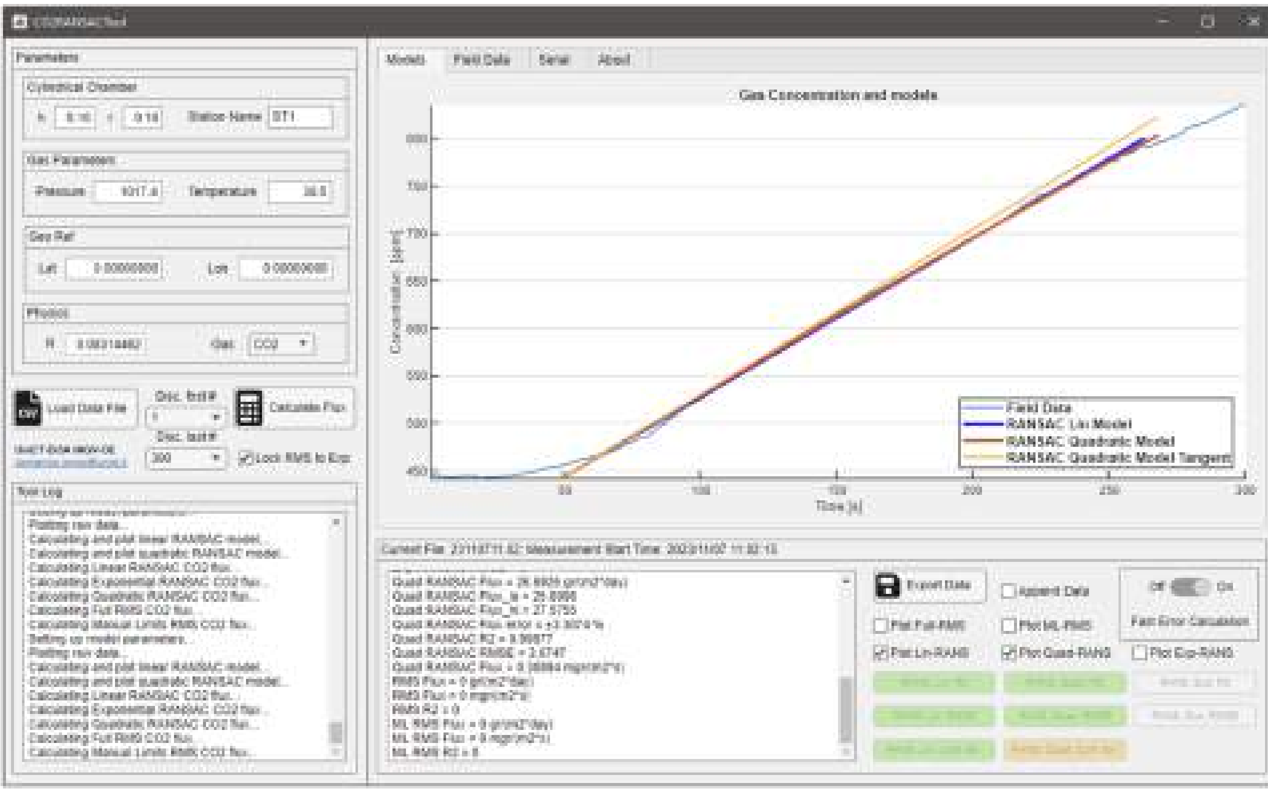

Fig. 4. Matlab® tool while processing a concentration dataset and comparing linear and quadratic models.

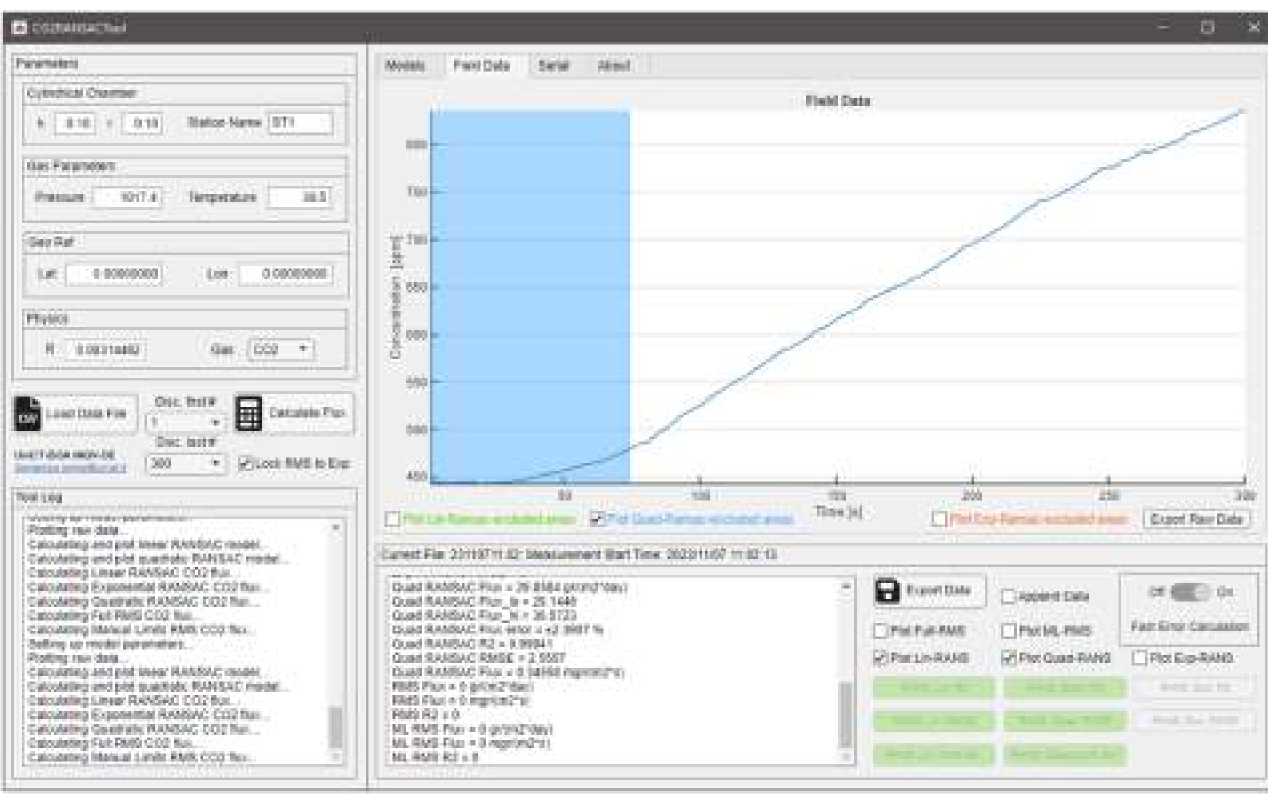

Fig. 5. Matlab® tool while processing a concentration dataset; RANSAC excluded data for quadratic model.

Second-order error sources:

- Temperature error: about ± 0.5 °C for the BME280 sensor.
- Pressure error: about ± 100 Pa for the BME280 sensor.
- Time measurement error: the MG2 data logger uses a DS3231 (Maxim / Analog Devices) real-time clock (RTC) to compute time

measurement. This silicon chip introduces an error of about ± 3.8 μs for each second.

- Chamber volume error: the volume of the chamber is designed not to saturate within the range of the considered fluxes throughout the entire sampling period (300 s). Beyond this, the chamber may undergo volume changes as a result of changes in ambient temperature.

With regard to first-order errors, particularly IRGA measurement errors, it is not possible to improve this performance without using a more expensive instrument. Regarding the standard gas used for calibration and its related accuracy, it must be considered that in this particular application, the focus is solely the variation in concentration measurements. Therefore, the effect of calibration gas accuracy on the final flux measurement can be neglected. Consequently, only the errors introduced by the mathematical models need to be investigated.

In order to validate the design and behavior of the measurement system presented in this work, considering all sources of error as an aggregate, a suitable experimental setup was designed and implemented. The experimental setup was based on a similar configuration [78]. The main idea was to obtain a constant gas flux from a porous soil and compare measurements to those obtained using a commercial instrument. The reference instrument used was the EGM-5 from PP Systems. The gas used was a certified mixture from SOL SpA (cert. ID: 16-P-57,840, expire: 08/2025) with the following composition, with ± 2 % tolerance with respect to each nominal value:

- Oxygen: 20.2 %;
- Carbon dioxide: 0.347 %;
- Nitrogen: complement.

The mixture was contained in a standard 10 L steel cylinder at a nominal pressure of 15 MPa. The cylinder pressure regulator was set to 0.2 MPa, and the flow was regulated to about 0.5 L min^{-1} or 1 L min^{-1} to consider two different flow levels. The flow meter / regulator used was a FR2000 series from Key Instruments, with a measurement range of (0.1 –1.0) L min^{-1}. This gas mixture flow was then sent to the bottom of a plastic bucket (35 cm diameter and 40 cm height) using perforated pipes to uniformly distribute the flow over all surfaces (Fig. 6). The bucket was then filled with commercially available dry inert sand consisting of a mixture of grains with a granulometry in the range (0 –6) mm.

Calibration tests were performed on three different days, following the same protocol while modifying some details to obtain the best possible performance, so only the last day data are reported. The gas was allowed to flow through the sand for approximately one hour to achieve a steady-state gas concentration in the sand. This condition arises from the mixing of the gas from the cylinder with the air contained in the sand, along with continuous mixing of this gas with atmospheric air. Once the steady-state condition was reached, measurements were alternated between the EGM-5 chamber and two different chambers under evaluation, named “POT3” and “POT4”. The EGM-5 was set to its maximum 120 s acquisition time, with the internal mixing fan activated. The systems under evaluation were set to a 300 s acquisition time.

Calibration results are reported in Fig. 7. The CO_2 flux measured by the chambers was calculated using a quadratic model on raw data of both systems (EGM-5 and the two chambers under test) and applying the RANSAC algorithm with 400 iterations. The bars represent the 2.5th percentile (2.5 %) and the 97.5th percentile (97.5 %), whereas the points represent the 50th percentile (50 %, median) of the CO_2 flux values.

The two levels (0.5 L min^{-1} and 1 L min^{-1}) of gas flow coming from the gas cylinder and measured by the Key Instruments fluxmeter, corresponded to an estimated mean CO_2 flux values on the sand surface, as measured by the chambers, of about 15 g m^{-2} day^{-1} and 54 g m^{-2} day^{-1} respectively, as average between the measurements of the different devices for each of the two flux levels, represented by the two red lines in Fig. 7.

The analysis of variance (ANOVA) applied to the median data did not show significant differences (p-level = 0.330) between the two devices in the measurement of the two flux levels (Table 3). First measurements were not taken into account in the analysis as taken with gas fluxes not yet stabilized. Some differences in median values between the two devices could be due to non-uniform flux from the sand and mainly related to the small diameter of the EGM-5 instrument compared to the chambers of the system under test; the latter are larger and can better integrate the soil flux from the bucket.

Moreover, a direct comparison of the raw data from the EGM-5 instrument and the two systems under test, showed that the rinse phase with fresh air pumped inside the chamber of the two systems, did not cause relevant soil depletion, as the dead band had a similar width, nor did it result to have gas leakage.

System performance is summarized in Table 3, considering all experiment repetitions reported in Fig. 7 for the two flux levels. The “mean flux” is the average of all median fluxes for the two considered levels and the different instruments used. The same applies to the

Fig. 6. Calibration experimental setup.

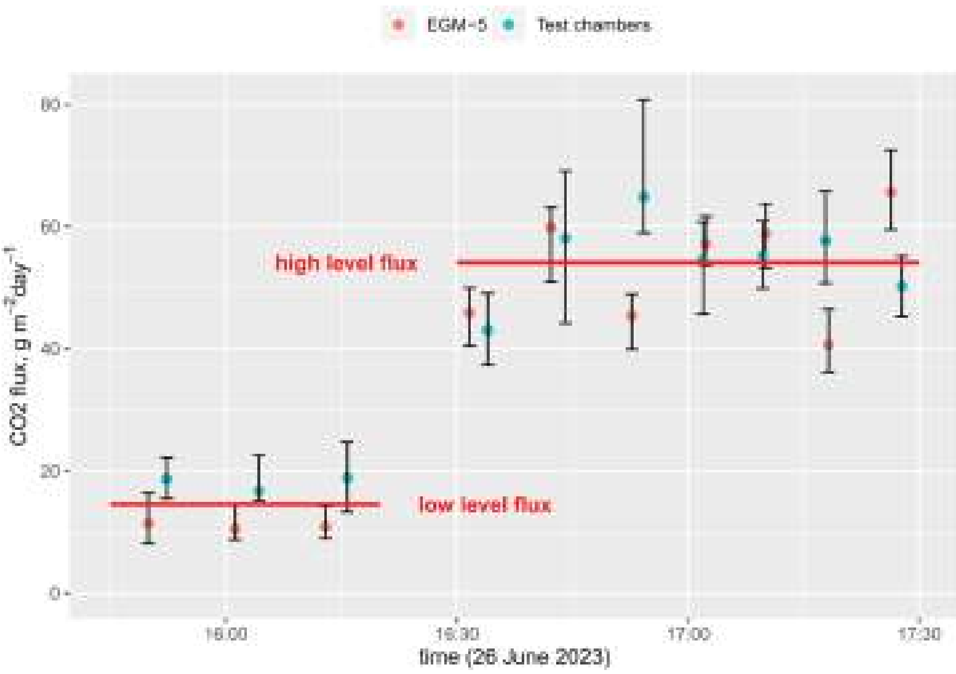

Fig. 7. Calibration results.

Table 3
Summary of calibration results (ns: differences not statistically significant between the two instruments for each flux level).

flux level	instrument	mean flux (g m^{-2} day^{-1})	standard deviation (g m^{-2} day^{-1})	coefficient of variation (%)
Low	EGM-5	10.95ns	0.43	3.9
	POT	18.09ns	1.19	6.6
High	EGM-5	53.34ns	9.28	17.4
	POT	54.82ns	6.84	12.5

"standard deviation" column. The last column represents the "coefficient of variation", calculated as in Eq. (6).

$$\text{coefficient of variation (\%)} = \frac{\text{standard deviation}}{\text{mean flux}} \times 100 \quad (6)$$

From Table 3 and Fig. 7, it is possible to see a good agreement between the reference instrument and the developed system, especially in the case of higher flux. In addition, the system under test showed a coefficient of variation of 12.5 % at high fluxes, lower than that of EGM-5 system (17.4 %). At high fluxes, the small chamber diameter of the EGM-5 system was more sensitive to inhomogeneity in gas flux coming out from the sand. This sensitivity can explain some differences compared to the measurements performed using the systems under test, which have a chamber with a larger diameter and can better integrate the total gas emission.

4. Measurements in case studies

In order to validate and improve the instrument, various field tests have been conducted since 2020. These trials allowed us to modify the system's behavior to achieve the best possible CO_2 time series throughout the measurement process. The main applications range from agronomy and volcanology to wastewater treatment plant monitoring. Below, the most relevant tests are briefly described. Some of these tests are ongoing; some are concluded and others will start as soon as possible. Detailed information about each application is or will be provided in dedicated papers.

4.1. Case study: CO_2 flux in a treatment wetland system

This section reports a multi-day dataset recorded in a TWs system for wastewater produced by the IKEA® retail store of Catania (Fig. 8), in the eastern part of Sicily (37° 26′ 48.30″ N, 15° 1′ 56.44″ E, WGS84), which also provides restaurant and bar services. Wastewater from toilets and food area are treated in a decentralized plant based on a screening unit and a sequential batch reactor designed for 30 m^3 day^{-1}. However, due to the high variability in wastewater hydraulic and organic loads related to customers incoming fluctuations (up to 45–50 m^3 day^{-1}), this system is integrated with a green infrastructure consisting in a hybrid TWs with one 400 m^2 horizontal subsurface flow wetland (HF), as a first unit, followed by two 530 m^2 vertical subsurface flow wetlands (VF1, VF2) in series. The latter are intermittently fed every 4 h (six times per day), while the HF unit is fed every 6 h (four times per day: 7:00 am – 1:00 pm – 7:00 pm – 1:00 am). The hybrid TWs has been in operation since 2014 with the aim to provide a polishing stage to the conventional system and to match the Italian limits for discharge in vulnerable areas [79]. Different species of macrophytes are present in the treatment units: HF is planted with *Phragmites australis* (Cav.) Trin. ex Steud., while VF1 and VF2 with *Cyperus papyrus* L., *Canna indica* L., *Typha latifolia* L. and *Iris pseudacorus* L., respectively. Further details are reported by Marzo et al. [80] and Ventura et al. [81].

Meteorological data recorded by the Catania weather station managed by SIAS (Sicilian Agro-meteorological Information Service) are typical of Mediterranean environments with an average rainfall for 2020 of about 780 mm and a mean annual temperature of 18.3 °C, ranging from a minimum of 4.3 °C up to a maximum of 32.7 °C.

The data were collected during a preliminary three-day monitoring campaign conducted over the third weekend of October 2020. In this regard, COVID-19-related rules and restrictions certainly influenced the ordinary operating conditions of the system. However, given the scope of the monitoring, this influence can be considered negligible. This continuous recording test has been conducted on a single sampling point of the second transect of the HF unit (Fig. 8), with dense vegetation.

In Fig. 9 the positive correlation between the CO_2 fluxes and the air temperature is evident (Pearson's coefficient of correlation = 0.70) and probably related to the increasing microbial respiration with the increasing temperature over the days, while eventual correlation with

Fig. 8. IKEA Store hybrid treatment wetlands (Catania, Sicily; 37° 26′ 48.30″ N, 15° 1′ 56.44″ E, WGS84). The red cross is the CO_2 sampling point in the HF unit (numbers are the piezometers that divide the unit in three transects: points 1–2–3 indicate the first transect; points 4–5–6 the second transect; points 7–8–9 the third transect). VF1, VF2 are the two vertical subsurface flow wetlands.

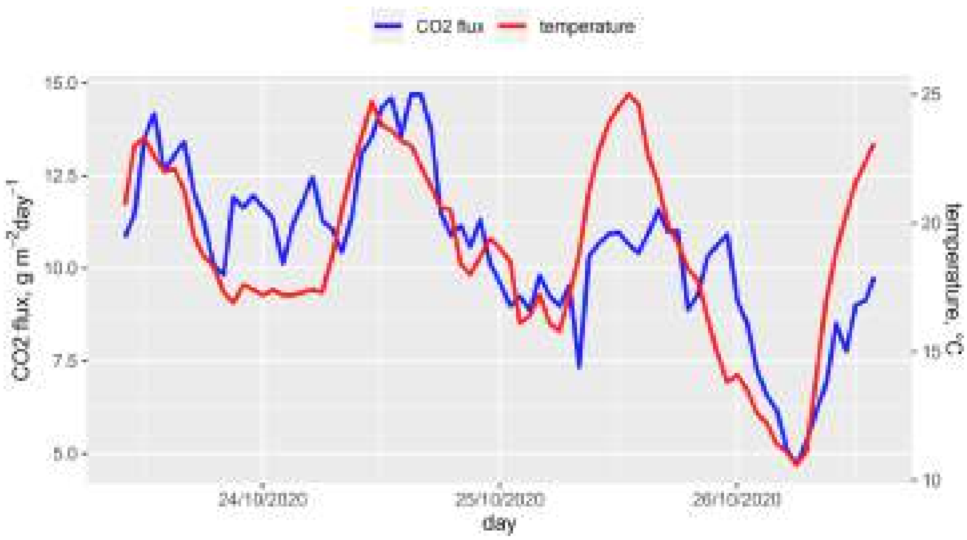

Fig. 9. CO_2 flux over multiple days and related environmental temperature measured at the IKEA Store hybrid treatment wetlands (Catania, Sicily).

wastewater input rate to the system should be investigated. In Fig. 10, trends can be considered representative of plant's biological cycling. The negative correlation between CO_2 environmental levels and air temperature is evident (Pearson's coefficient of correlation = −0.72) and related to the process of CO_2 absorption during the photosynthesis in the daytime and the biogenic release during the respiration in the night.

In order to shed further light on this issue, as in the literature [82,83] there is no consensus on whether TWs are source or sink of GHGs, more consistent sampling campaigns for CO_2 flux monitoring at the hybrid TWs system of the IKEA Store of Catania started in March 2024 and are currently ongoing on a monthly basis, together with water quality and hydraulic parameters (i.e., flows, hydraulic retention time, saturated hydraulic conductivity).

4.2. *Case study: accumulation chamber test in Aurora, a fumarolic ice cave on Mt. Melbourne caldera, Antarctica*

Under the auspices of PNRA, the Italian Antarctic Program, during the XXXVIII Antarctic campaign, one accumulation chamber similar to that presented here, was deployed for a test experiment inside a Fumarolic Ice Cave (FIC), named Aurora, located on a side of Mt. Melbourne caldera. Mt. Melbourne is a quiescent volcano close to the Italian Mario Zucchelli Station (MZS), as well as Jan Bogo (KOPRI program - South Korea) and Gondwana (GANOVEX program - Germany), and the new Chinese station, their fifth one in Antarctica.

Since 2016, three different PNRA projects have focused their activities on volcanic studies on Mt. Melbourne: Icevolc, MIMIC, and the new Italian VOLCanological observatory in ANtarctica (I-Volcan). The

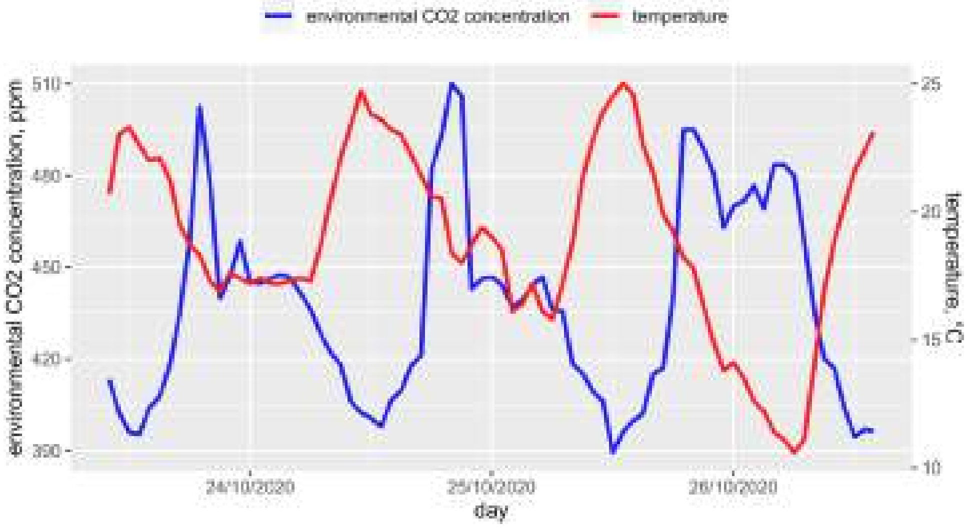

Fig. 10. Environmental CO_2 background concentration over multiple days and related environmental temperature measured at the IKEA Store hybrid treatment wetlands (Catania, Sicily).

volcano's proximity to scientific stations, its position under several main Antarctic flight routes, and the last presumed eruption, dated to about 150 years ago, lead to the idea of preparing a volcanic surveillance network to analyze the fumarolic activities manifested on the summit caldera.

FICs have formed on this caldera in correspondence to several fumarolic areas, due to the thermal erosion of the snow layers covering the entire caldera, which in some points are tens of meters thick. Water vapor in these FICs, with temperature ranging from 10 °C to >40 °C near the soil close to the fumaroles, easily melts the ice and snow mantle above. The water vapor flows up from the fumaroles and reaches the emission point in the external atmosphere, where forms frost suddenly, creating a tower-shaped chimney called Ice Tower. These Ice Towers often provide access to the FICs, sometimes easily and other times requiring rope and speleo-alpinistic approaches.

Inside these caves, it is possible to conduct various experiments and perform geophysical and geochemical analyses and measurements. While the harsh external environment poses serious challenges for maintaining the instruments, the temperature inside the caves is relatively stable, averaging around 0 °C, with no storms that are devastating outside, especially during winter. Consequently, different monitoring instruments have been deployed inside the FICs, including the accumulation chamber described in this work (Fig. 11).

The geochemical station installed in the Aurora FIC recorded a time series of data, including CO_2 soil fluxes and concentration from the automatic accumulation chamber (Fig. 12). The station was activated twice a day, and the plotted data were obtained through post-processing of the raw data gathered and stored in the server database. The data were transmitted from the station via radio connection to a central server at MZS. As underlined by Larocca et al. [84], there were some brief periods when the atmospheric CO_2 concentration inside the cave was high, leading to negative soil flux values [85,86]. According to Fik's law, CO_2 soil flux and CO_2 air concentration were negatively correlated (Pearson's coefficient of correlation = −0.66).

The ice cave itself acts as a gas integrator, with relatively hot gases from different fumarole areas flowing from the bottom to the top, similar to a chimney effect. These gases are diluted with air entering through cracks in the ice mantle at the lower part of the cave. At low airspeed (measured near the CO_2 flux measuring instrument inside the cave), there is less dilution, resulting in higher CO_2 concentration in the air than in the soil, leading in negative CO_2 fluxes. Conversely, at higher airspeed, the CO_2 in the air is more diluted, resulting in positive fluxes. Again, CO_2 soil flux and air speed were negatively correlated (Pearson's coefficient of correlation = −0.52).

4.3. Case study: accumulation chamber test in Santa Venerina – Mt. Etna

Recently, a new monitoring setup has been deployed on Mt. Etna

Fig. 11. The developed accumulation chamber during Aurora cave monitoring test among other geochemical instrumentation.

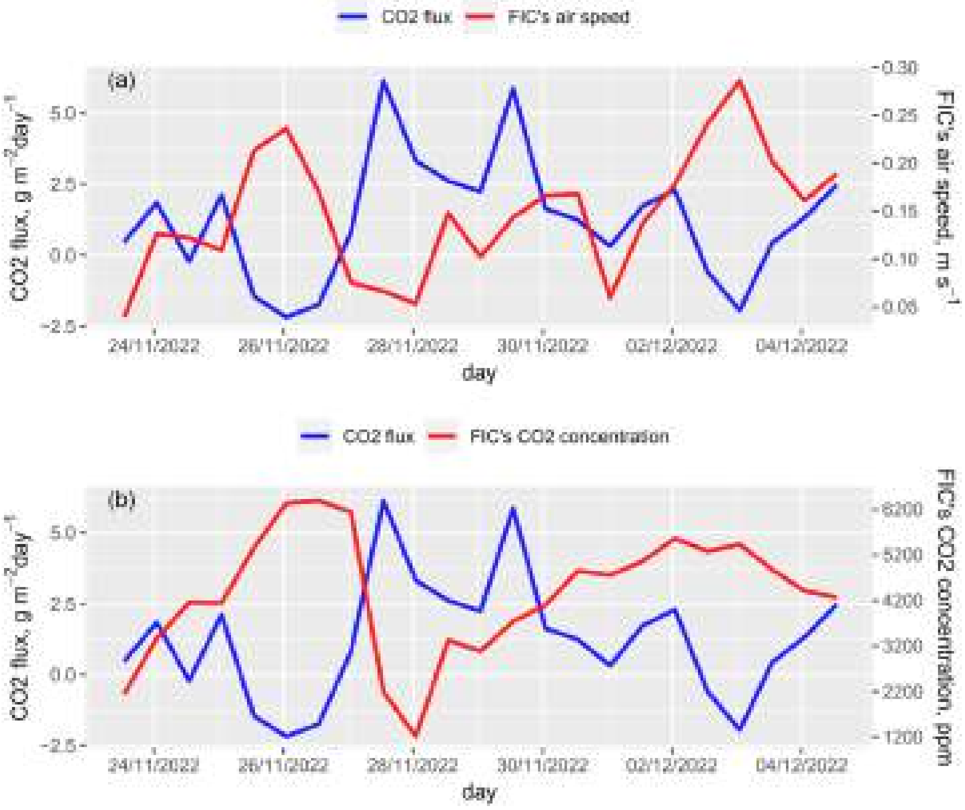

Fig. 12. Time series of CO_2 flux in comparison to air speed (a) and CO_2 concentration (b), recorded by the multi-gas station installed in the Aurora FIC during 23 November–4 December 2022.

(with station name "POT4"). Near the village of Santa Venerina, the presence of a seismogenic fault (SV1) is known to be correlated with Etna volcano dynamics [87–89]. The aim was to assess variations in CO_2 fluxes from the soil in this area. Additionally, along the same fault, the INGV (Istituto Nazionale di Geofisica e Vulcanologia) has four other geochemical monitoring stations. They are named "Primoti", "SV1", "P78" and "Ponteferro" (Fig. 13). This setup will enable the comparison of acquired data with other trusted measurements.

At the test site (Fig. 13, 37° 41′ 41.50″ N, 15° 7′ 43.09″ E, WGS84), a preliminary discrete survey was conducted using the developed system,

Fig. 13. Location of test site (POT4, 37° 41′ 41.50″ N, 15° 7′ 43.09″ E, WGS84) and reference stations around SV1 fault.

revealing a mean background CO_2 flux of about 20 g m^{-2} day^{-1}. This flux value was consistent with the expected values reported by other stations in this area, which are distant from volcanic or seismic events.

Therefore, like in different peripheral areas of Etna, the increase in CO_2 emissions can often be considered of volcanic origin as demonstrated in Messina et al., [90] and correlated with a variation in volcanic activity [14,16,22].

4.4. Case study: CO_2 flux in Mediterranean orange orchard

This section reports a subset of the results obtained from an intensive soil CO_2 monitoring activity conducted in an orange orchard (*Citrus sinensis* (L.) Osbeck cv "Tarocco Sciara") subjected to different soil management (bare versus mulch) and irrigation practices (regulated deficit irrigation, versus full irrigation) [91,92].

In particular, the orchard is managed by the Italian Council for Agricultural Research and Agricultural Economics Analyses (CREA-OFA) and is located in the insular part of Italy (Eastern Sicily, Lentini, SR, 37° 20′ 12.65″ N, 14° 53′ 33.04″ E, WGS84). The study area is characterized by a semi-arid Mediterranean climate, with warm and dry irrigation seasons. During the years 2010–2021, the mean yearly air temperature and reference evapotranspiration values were 18.2 °C and 1264 mm, respectively. Annual precipitation in the same period was 587 mm. The agrometeorological data was provided by a weather station located about 2 km from the study site and managed by the Sicilian Agro-meteorological Information Service (SIAS).

The soil CO_2 monitoring was carried out monthly in the morning period (between 9:00 am and 1:00 pm) during the spring seasons 2022 and 2023, without using the soil collar. Specifically, two types of soil CO_2 surveys were performed at the study site, both in discontinuous and continuous acquisition mode. The measurements were conducted at 24 sample points; see more details in [91], where all the measurements were done using the instrument presented in this work.

No significant differences were obtained under the proposed soil management practices and irrigation regimes, suggesting that the application of organic mulching may allow the addition of organic matter to the soil without increasing soil CO_2 fluxes. In addition, an overall significant increase in soil CO_2 was observed in 2023 (p-value of 0.02, Tukey test). To better understand the mechanisms of soil CO_2 emission related to strong interactions between soil, plant roots exudates, soil fungi and bacteria, it is necessary to conduct long-term soil CO_2 monitoring.

5. Conclusion

The necessity of measuring CO_2 emissions from soils and other artificial sources has become evident in various scientific and industrial fields. Various methods for measuring CO_2 flux are available and when the gas flux from soil or water surfaces is the target, one of the most commonly used methods is the accumulation chamber technique.

Various devices are commercially available for measuring CO_2 flux, although not all are suitable for use in very harsh conditions, such as those found in volcanic environments. Additionally, while some devices may be suitable for specific applications like discrete surveys, they may not be appropriate for continuous monitoring over extended periods. Many of these devices utilize mechanical moving parts to reset the initial chamber gas condition, leading to high costs and the need for frequent maintenance due to mechanical breakage failures. These issues, particularly in the context of precision agriculture or volcanology, limit the widespread adoption of these instruments, thereby restricting the benefits of using multiple instruments in large areas. For instance, different tools may be required to assess best practices across large areas with varying soil and water management techniques.

The proposed instrument, on the other hand, utilizes no mechanical moving parts, resulting in reduced maintenance requirements and lower production costs. The system was designed considering both the state-of-the-art of existing systems and real-field constraints, particularly regarding continuous monitoring for extended periods in fully automated mode. The presence of fans for mixing the gas in the chamber is not needed in the proposed instrument, because both the dead band of CO_2 data stream and the resulting fluxes are in good agreement with those of the commercial instrument used for reference, equipped with a mixing fan. A specially developed post-processing software [74] has been created in Matlab® to simplify the evaluation of CO_2 flux from raw data collected by the onboard data logger. Additionally, a graphical user interface accessible via smartphone WiFi connection, has been developed to enable real-time instrument readout and control. This application is compatible with most popular web browsers (Chrome, Firefox, Microsoft Edge and similar) and operating systems, eliminating the need for installing specific software on smartphones or PCs.

To validate system performance, a specially designed test bench was utilized, employing a certified gas mixture with known CO_2 concentration. The developed system was compared to a commercial system (EGM-5 from PP Systems), and measurements were found to be in good agreement. The coefficient of variation under laboratory conditions was lower than 12 %, considering various flux regimes typical of agronomical applications and also near the common background values in volcanological applications. This result is particularly interesting in volcanological applications, where significant information arises from strong variations with respect to background levels.

The developed instrument was also tested in real on-field applications, including agriculture, wastewater treatment and volcanology, in correlation with studies on GHG. Some of these applications were described in detail, and preliminary results were presented. Each of these applications represents an ongoing study in their respective fields, and detailed results have been or will be presented in dedicated publications.

All these field tests have led to improvements in the system, highlighting critical issues and enabling the resolution of related problems. It is worth noting that by replacing the used gas analyzer, the same instrument can be adapted for monitoring other GHG, such as methane. Also, the measurement volume can be easily changed with other of different height. The developed system is currently upgradable and, thanks to careful prototype development, can be engineered and offered as a commercial system for approximately €5000, including real time and post-processing software. However, assembling its bare components in-house can cost as low as €500. Potential buyers can be research center or farm owners that wish to implement some precision agricultural paradigm. Even operators of sewage treatment plants can be interested, in case they wish to monitor plant GHG emissions. The system has an ongoing patent procedure.

CRediT authorship contribution statement

Domenico Longo: Writing – review & editing, Writing – original draft, Visualization, Supervision, Software, Methodology, Formal analysis, Conceptualization. **Serena Guarrera:** Writing – original draft. **Delia Ventura:** Writing – original draft. **Emanuele Cerruto:** Writing – review & editing, Writing – original draft, Visualization, Formal analysis. **Salvatore Roberto Maugeri:** Writing – original draft. **Gaetano Giudice:** Writing – review & editing, Writing – original draft, Supervision, Software, Methodology, Formal analysis, Conceptualization.

Declaration of competing interest

The authors declare that they have no known competing financial interests or personal relationships that could have appeared to influence the work reported in this paper.

Acknowledgments

This work has been partially funded by:

- European Union (NextGeneration EU), through the MUR-PNRR project SAMOTHRACE (ECS00000022).

- The Italian Ministry of Universities and Research for funding, within the Progetti di Rilevante Interesse Nazionale - PRIN 2017 initiative; project INtegrated Computer modeling and monitoring for Irrigation Planning in Italy (INCIPIT).

- The project "Miglioramento delle produzioni agroalimentari mediterranee in condizioni di carenza di risorse idriche –WATER4AGRIFOOD". Cod. progetto: ARS01_00825; cod. CUP: B64I20000160005, "PON "RICERCA E INNOVAZIONE" 2014–2020.

- The research project "Innovazioni nell'ottimizzazione delle risorse idriche per l'irrigazione di colture da pieno campo" (DICrops) Linea 2 Ricerca di Ateneo2019–21 (Università degli Studi di Catania).

- This research was funded by the University of Catania with the research projects "Sostenibilità ed innovazioni della ricerca in agricoltura, alimentazione e ambiente—WP 6: Monitoraggio ambientale, Meccanica e Meccanizzazione Sostenibile nell'Agricoltura Mediterranea", premialità Linea 2 PIACERI.

- European Union –FSE-REACT EU, PON "Research & Innovation" 2014–2020, Action IV.6, DM 1062/2021 (CUP E61B21004280005).

We thank IKEA® Retail Italia of Catania and its technical personnel for their comprehensive availability and assistance during the measurement activities at the site. Special thanks to Dr. S. Giammanco (INGV-OE) for kindly providing the reference system EGM-5 from PP Systems and related support.

Data availability

Data will be made available on request.

References

[1] C.D. Keeling, The Concentration and Isotopic Abundances of Carbon Dioxide in the Atmosphere, in: Tellus, 12, Stockholm University Press, 1960, pp. 200–203, https://doi.org/10.1111/j.2153-3490.1960.tb01300.x.

[2] WMO, World Meteorological Organization (2025) https://wmo.int/.

[3] SERC, Smithsonian, Environmental Research Center (2025). https://serc.si.edu/gcrew/CO2.

[4] DCO, Deep Carbon Observatory (2025). https://deepcarbon.science/.

[5] S. Inguaggiato, M.P Jácome Paz, A. Mazot, H. Delgado Granados, C. Inguaggiato, F. Vita, CO_2 output discharged from Stromboli Island (Italy), in: Chemical Geology, 339, Elsevier BV, 2013, pp. 52–60, https://doi.org/10.1016/j.chemgeo.2012.10.008.

[6] S. Inguaggiato, F. Vita, M. Cangemi, C. Inguaggiato, L. Calderone, The Monitoring of CO_2 Soil Degassing as Indicator of Increasing Volcanic Activity: the Paroxysmal Activity at Stromboli Volcano in 2019-2021, Geosciences. (Basel) 11 (4) (2021) 169, https://doi.org/10.3390/geosciences11040169.

[7] M.L. Carapezza, S. Inguaggiato, L. Brusca, M. Longo, Geochemical precursors of the activity of an open-conduit volcano: The Stromboli 2002-2003 eruptive events, in: Geophysical Research Letters, 31, American Geophysical UnionAGU, 2004, https://doi.org/10.1029/2004gl019614.

[8] C. Cardellini, G. Chiodini, F. Frondini, R. Avino, E. Bagnato, S. Caliro, M. Lelli, A. Rosiello, Monitoring diffuse volcanic degassing during volcanic unrests: the case of Campi Flegrei (Italy), in: Scientific Reports, 7, Springer Science and Business Media LLC, 2017, https://doi.org/10.1038/s41598-017-06941-2.

[9] D. Granieri, G. Chiodini, W. Marzocchi, R. Avino, Continuous monitoring of CO_2 soil diffuse degassing at Phlegraean Fields (Italy): influence of environmental and volcanic parameters, in: Earth and Planetary Science Letters, 212, Elsevier BV, 2003, pp. 167–179, https://doi.org/10.1016/s0012-821x (03)00232-2.

[10] M.P. Jácome - Paz, Y. Taran, S. Inguaggiato, N. Collard, CO_2 flux and chemistry of El Chichón crater lake (México) in the period 2013-2015: Evidence for the enhanced volcano activity, Geophys. Res. Lett. 43 (1) (2016) 127, https://doi.org/10.1002/2015GL066354.

[11] M.P. Jácome - Paz, H.D. Granados, X. Pérez-Campos, R. Espinasa-Pereña, R. Campion, Diffuse Degassing Baseline in Parícutin volcano and Michoacán-Guanajuato monogenetic volcanic field, México, Journal of Volcanology and Geothermal Research (2022) 425, https://doi.org/10.1016/j.jvolgeores.2022.107534.

[12] M.C. Lamberti, A. Chiodi, M. Agusto, R. Filipovich, A. Massenzio, W. Báez, F. Tassi, O. Vaselli, Carbon dioxide diffuse degassing as a tool for computing the thermal energy release at Cerro Blanco Geothermal System, Southern Puna (NW Argentina), In Journal of South American Earth Sciences 105 (2021), https://doi.org/10.1016/j.jsames.2020.102833.

[13] D. Pérez-Zárate, E. Santoyo, M.P. Jácome-Paz, M. Guevara, F. Guerero, D. Yáñez-Dávila, G. Santos-Raga, Soil CO_2 fluxes measured in the Acoculco Geothermal System, Mexico: Baseline emissions from a long-term prospection programme, Geochemistry 84 (2) (2024), https://doi.org/10.1016/j.chemer.2024.126112.

[14] A. Aiuppa, M. Bitetto, D. Delle Donne, F.P. La Monica, G. Tamburello, D. Coppola, M. Della Schiava, L. Innocenti, G. Lacanna, M. Laiolo, F. Massimetti, M. Pistolesi, M.C. Silengo, M. Ripepe, Volcanic CO_2 tracks the incubation period of basaltic paroxysms. Science Advances 7, American Association for the Advancement of Science (AAAS), 2021, https://doi.org/10.1126/sciadv.abh0191.

[15] C. Caudron, A. Mazot, A. Bernard, Carbon dioxide dynamics in Kelud volcanic lake, Journal of Geophysical Research (Solid Earth) 117 (2012), https://doi.org/10.1029/2011JB008806.

[16] S. Gurrieri, M. Liuzzo, G. Giudice, Continuous monitoring of soil CO_2 flux on Mt. Etna: The 2004-2005 eruption and the role of regional tectonics and volcano tectonics, in: Journal of Geophysical Research: Solid Earth, 113, American Geophysical UnionAGU, 2008, https://doi.org/10.1029/2007jb005003.

[17] J.M.L. Salazar, N.M. Pérez, P.A. Hernández, T. Soriano, F. Barahona, R. Olmos, R. Cartagena, D.L. López, R.N. Lima, G. Melián, I. Galindo, E. Padrón, H. Sumino, K. Notsu, Precursory diffuse carbon dioxide degassing signature related to a 5.1 magnitude earthquake in El Salvador, Central America, in: Earth and Planetary Science Letters, 205, Elsevier BV, 2002, pp. 81–89, https://doi.org/10.1016/s0012-821x(02)01014-2.

[18] H. Shinohara, A. Aiuppa, G. Giudice, S. Gurrieri, M. Liuzzo, Variation of H_2O/CO_2 and CO_2/SO_2 ratios of volcanic gases discharged by continuous degassing of Mount Etna volcano, Italy, J. Geophys. Res. 113 (2008), https://doi.org/10.1029/2007JB005185.

[19] M. Camarda, S. Gurrieri, M. Valenza, CO_2 flux measurements in volcanic areas using the dynamic concentration method: Influence of soil permeability, in: Journal of Geophysical Research: Solid Earth, 111, American Geophysical UnionAGU, 2006, https://doi.org/10.1029/2005jb003898.

[20] S. Gurrieri, M. Valenza, Gas transport in natural porous medium: a method for measuring soil CO_2 flows from the ground in volcanic and geothermal areas, Rend. Soc. Ital. Mineral. Petrol. 43 (1988) 1151–1158.

[21] S. Inguaggiato, F. Vita, M. Cangemi, L. Calderone, Increasing Summit Degassing at the Stromboli Volcano and Relationships with Volcanic Activity (2016-2018), in: Geosciences, 9, MDPI AG, 2019, p. 176, https://doi.org/10.3390/geosciences9040176.

[22] M. Liuzzo, S. Gurrieri, G. Giudice, G. Giuffrida, Ten years of soil CO_2 continuous monitoring on Mt. Etna: Exploring the relationship between processes of soil degassing and volcanic activity, in: Geochemistry, Geophysics, Geosystems, 14, American Geophysical Union (AGU), 2013, pp. 2886–2899, https://doi.org/10.1002/ggge.20196.

[23] F. Viveiros, C. Cardellini, T. Ferreira, S. Caliro, G. Chiodini, C. Silva, Soil CO2 emissions at Furnas volcano, São Miguel Island, Azores archipelago: Volcano monitoring perspectives, geomorphologic studies, and land use planning application, in: Journal of Geophysical Research: Solid Earth, 115, American Geophysical UnionAGU, 2010, https://doi.org/10.1029/2010jb007555.

[24] B. Bond-Lamberty, A. Thomson, A Global Database of Soil Respiration data. In Biogeosciences, 7, Copernicus GmbH, 2010, pp. 1915–1926, https://doi.org/10.5194/bg-7-1915-2010.

[25] P. Shao, H. He, X. Zhang, H. Xie, X. Bao, C. Liang, Responses of microbial residues to simulated climate change in a semiarid grassland, in: Science of The Total Environment, 644, Elsevier BV, 2018, pp. 1286–1291, https://doi.org/10.1016/j.scitotenv.2018.07.055.

[26] K. Wang, A. Bastos, P. Ciais, X. Wang, C. Rödenbeck, P. Gentine, F. Chevallier, V. W. Humphrey, C. Huntingford, M. O'Sullivan, S.I. Seneviratne, S. Sitch, S. Piao, Regional and seasonal partitioning of water and temperature controls on global land carbon uptake variability, in: Nature Communications, 13, Springer Science and Business Media LLC, 2022, https://doi.org/10.1038/s41467-022-31175-w.

[27] J. Jian, C. Gough, D. Sihi, A.M. Hopple, B. Bond-Lamberty, Collar Properties and Measurement Time Confer Minimal Bias Overall on Annual Soil Respiration Estimates in a Global Database, in: Journal of Geophysical Research: Biogeosciences, 125, American Geophysical UnionAGU, 2020, https://doi.org/10.1029/2020jg006066.

[28] G. Fischer, L.M. Melgarejo, H.E. Balaguera-López, Revisión del impacto de concentraciones elevadas de CO_2 sobre frutales en la era del cambio climático, in: Ciencia & Tecnología Agropecuaria, 23, Corporacion Colombiana de Investigacion Agropecuaria (Corpoica), 2022, https://doi.org/10.21930/rcta.vol23_num2_art:2475.

[29] European Commission. Directorate General for the Environment, Soil: the hidden part of the climate cycle, Publications Office (2011), https://doi.org/10.2779/30669.

[30] M. Reichstein, C. Beer, Soil respiration across scales: The importance of a model–data integration framework for data interpretation, in: Journal of Plant Nutrition and Soil Science, 171, Wiley, 2008, pp. 344–354, https://doi.org/10.1002/jpln.200700075.

[31] M.G. Ryan, B.E. Law, Interpreting, measuring, and modeling soil respiration, Springer Science and Business Media LLC 73 (1) (2005) 3–27, https://doi.org/10.1007/s10533-004-5167-7.

[32] M. Huang, X. Chen, A.A. Degen, R. Guo, T. Zhang, B. Luo, H. Li, J. Zhao, Z. Shang, Nitrogen addition stimulated soil respiration more so than carbon addition in alpine meadows, in: Environmental Research, 233, Elsevier BV, 2023 116501, https://doi.org/10.1016/j.envres.2023.116501.

[33] Ü. Mander, G. Dotro, Y. Ebie, S. Towprayoon, C. Chiemchaisri, S.F. Nogueira, B. Jamsranjav, K. Kasak, J. Truu, J. Tournebize, W.J. Mitsch, Greenhouse gas emission in constructed wetlands for wastewater treatment: a review, in: Ecological Engineering, 66, Elsevier BV, 2014, pp. 19–35, https://doi.org/10.1016/j.ecoleng.2013.12.006.

[34] EPA, 2012 U.S, Greenhouse Gas Inventory Report (2012). https://www.nrc.gov/docs/ML1428/ML14282A280.pdf.
[35] E.A. Davidson, D. Kanter, Inventories and scenarios of nitrous oxide emissions, In Environmental Research Letters 9 (10) (2014) 105012, https://doi.org/10.1088/1748-9326/9/10/105012. Issue.
[36] D. Ventura, M. Ferrante, C. Copat, A. Grasso, M. Milani, A. Sacco, F. Licciardello, G. L. Cirelli, Metal removal processes in a pilot hybrid constructed wetland for the treatment of semi-synthetic stormwater, in: Science of The Total Environment, 754, Elsevier BV, 2021 142221, https://doi.org/10.1016/j.scitotenv.2020.142221.
[37] E. Ranieri, G. D'Onghia, F. Ranieri, L. Lopopolo, S. Gregorio, A.C. Ranieri, Performance of wastewater treatment plants in emission of greenhouse gases, in: Bioresource Technology, 404, Elsevier BV, 2024 130897, https://doi.org/10.1016/j.biortech.2024.130897.
[38] S. Wang, X. Li, M. Ji, J. Zhang, M. Tanveer, Z. Hu, Is constructed wetlands carbon source or carbon sink? Case analysis based on life cycle carbon emission accounting, in: Bioresource Technology, 388, Elsevier BV, 2023 129777, https://doi.org/10.1016/j.biortech.2023.129777.
[39] Y. Wang, W. Gao, L. Lv, X. Ma, Z. Ren, L. Sun, X. Liu, P. Wang, Z. Sun, Y. Tian, G. Zhang, Comprehensive carbon footprint analysis of wastewater treatment: a case study of modified cyclic activated sludge technology for low carbon source urban wastewater treatment, in: Science of The Total Environment, 923, Elsevier BV, 2024 171550, https://doi.org/10.1016/j.scitotenv.2024.171550.
[40] M. El-Fadel, M. Massoud, Methane emissions from wastewater management, in: Environmental Pollution, 114, Elsevier BV, 2001, pp. 177–185, https://doi.org/10.1016/s0269-7491(00)00222-0.
[41] L. Huang, H. Li, Y. Li, Greenhouse gas accounting methodologies for wastewater treatment plants: a review, in: Journal of Cleaner Production, 448, Elsevier BV, 2024 141424, https://doi.org/10.1016/j.jclepro.2024.141424.
[42] T.K.L. Nguyen, H.H. Ngo, W.S. Guo, S.W. Chang, D.D. Nguyen, L.D. Nghiem, T. V. Nguyen, A critical review on life cycle assessment and plant-wide models towards emission control strategies for greenhouse gas from wastewater treatment plants, in: Journal of Environmental Management, 264, Elsevier BV, 2020 110440, https://doi.org/10.1016/j.jenvman.2020.110440.
[43] C. Maucieri, A.C. Barbera, J. Vymazal, M. Borin, A review on the main affecting factors of greenhouse gases emission in constructed wetlands, in: Agricultural and Forest Meteorology, 236, Elsevier BV, 2017, pp. 175–193, https://doi.org/10.1016/j.agrformet.2017.01.006.
[44] L. Li, H. Xu, Q. Zhang, Z. Zhan, X. Liang, J. Xing, Estimation methods of wetland carbon sink and factors influencing wetland carbon cycle: a review, in: Carbon Research, 3, Springer Science and Business Media LLC, 2024, https://doi.org/10.1007/s44246-024-00135-y.
[45] T.P. Fischer, A. Aiuppa, AGU Centennial Grand Challenge: Volcanoes and deep carbon global CO_2 emissions from subaerial volcanism—Recent progress and future challenges, Geochem. Geophys. Geosyst. 21 (3) (2020), https://doi.org/10.1029/2019GC008690.
[46] M. Zaman, L. Heng, C. Müller (Eds.), Measuring Emission of Agricultural Greenhouse Gases and Developing Mitigation Options using Nuclear and Related Techniques, Springer International Publishing, 2021. 10.1007/978-3-030-55396-8.
[47] G. Chiodini, R. Cioni, M. Guidi, B. Raco, L. Marini, Soil CO_2 flux measurements in volcanic and geothermal areas, In Applied Geochemistry 13 (5) (1998) 543–552, https://doi.org/10.1016/s0883-2927(97)00076-0.
[48] W. Al Hamwi, M. Dubbert, J. Schaller, M. Lück, M. Schmidt, M. Hoffmann, A low-cost, automatic soil-plant-atmosphere enclosure system to investigate CO2 and evapotranspiration flux dynamics, Biogeosciences 21 (24) (2024) 5639–5651, https://doi.org/10.5194/bg-21-5639-2024.
[49] E. Forbes, V. Benenati, S. Frey, M. Hirsch, G. Koech, G. Lewin, J.N. Mantas, K. Caylor, Fluxbots: a method for building, deploying, collecting and analyzing data from an array of inexpensive, autonomous soil carbon flux chambers, Journal of Geophysical Research: Biogeosciences 128 (2023) e2023JG007451, https://doi.org/10.1029/2023JG007451.
[50] R. Macagga, M. Asante, G. Sossa, D. Antonijević, M. Dubbert, M. Hoffmann, Validation and field application of a low-cost device to measure CO_2 and evapotranspiration (ET) fluxes, Atmos. Meas. Tech. 17 (2024) 1317–1332, https://doi.org/10.5194/amt-17-1317-2024.
[51] L. Xu, M.D. Furtaw, R.A. Madsen, R.L. Garcia, D.J. Anderson, D.K. McDermitt, On maintaining pressure equilibrium between a soil CO_2 flux chamber and the ambient air, in: Journal of Geophysical Research: Atmospheres, 111, American Geophysical UnionAGU, 2006, https://doi.org/10.1029/2005jd006435.
[52] ADC Bioscientific Ltd, ACE (2025). https://www.adc.co.uk/products/ace-automated-soil-co2-exchange-system/.
[53] LiCOR, Li-8200 (2025), https://www.licor.com/env/products/soil-flux/8200-104.
[54] PP Systems, CFlux-1 (2025), https://ppsystems.com/soil-and-canopy-flux/.
[55] West Systems (2025), https://www.westsystems.eu/en/instrumentation/diffuse-emission/continuous-monitoring..
[56] S. Barbagallo, S. Barresi, G.L. Cirelli, M. Ferrante, G. Giudice, D. Longo, M. Milani, Trattamenti naturali per la depurazione delle acque reflue agrumarie. Nuovi prodotti dalla trasformazione agroindustriale di frutti da colture mediterranee e gestione sostenibile dei sottoprodotti, AA. VV. CSEI Catania, 2023, pp. 218–243. https://hdl.handle.net/20.500.11769/590331.
[57] J.M. Norman, C.J. Kucharik, S.T. Gower, D.D. Baldocchi, P.M. Crill, M. Rayment, K. Savage, R.G. Striegl, A comparison of six methods for measuring soil-surface carbon dioxide fluxes, in: Journal of Geophysical Research: Atmospheres, 102, American Geophysical UnionAGU, 1997, pp. 28771–28777, https://doi.org/10.1029/97jd01440.
[58] R.W. Healy, R.G. Striegl, T.F. Russell, G.L. Hutchinson, G.P. Livingston, Numerical Evaluation of Static-Chamber Measurements of Soil-Atmosphere Gas Exchange: Identification of Physical Processes, in: Soil Science Society of America Journal, 60, Wiley, 1996, pp. 740–747, https://doi.org/10.2136/sssaj1996.03615995006000030009x.
[59] A. Heinemeyer, N.P. McNamara, Comparing the closed static versus the closed dynamic chamber flux methodology: Implications for soil respiration studies, in: Plant and Soil, 346, Springer Science and Business Media LLC, 2011, pp. 145–151, https://doi.org/10.1007/s11104-011-0804-0.
[60] E.T. Kanemasu, W.L. Powers, J.W. Sij, Field chamber measurement of CO_2 flux from soil surface, Soil. Sci. 118 (4) (1974) 233–237.
[61] PP Systems,, SBA-5 datasheet (2025). https://ppsystems.com/download/technical_manuals/800811-SBA5_Operation_V106.pdf.
[62] M. Pavelka, M. Acosta, R. Kiese, N. Altimir, C. Brümmer, P. Crill, E. Darenova, R. Fuß, B. Gielen, A. Graf, L. Klemedtsson, A. Lohila, B. Longdoz, A. Lindroth, M. Nilsson, S.M. Jiménez, L. Merbold, L. Montagnani, M. Peichl, W. Kutsch, Standardisation of chamber technique for CO_2, N_2O and CH_4 fluxes measurements from terrestrial ecosystems, in: International Agrophysics, 32, Walter de Gruyter GmbH, 2018, pp. 569–587, https://doi.org/10.1515/intag-2017-0045.
[63] A.R. Pedersen, S.O. Petersen, K. Schelde, A comprehensive approach to soil-atmosphere trace-gas flux estimation with static chambers, in: European Journal of Soil Science, 61, Wiley, 2010, pp. 888–902, https://doi.org/10.1111/j.1365-2389.2010.01291.x.
[64] P. Rochette, N.S. Eriksen-Hamel, Chamber Measurements of Soil Nitrous Oxide Flux: Are Absolute Values Reliable?, in: Soil Science Society of America Journal, 72 Wiley, 2008, pp. 331–342, https://doi.org/10.2136/sssaj2007.0215.
[65] C. Jiang, G. Yu, G. Cao, Y. Li, S. Zhang, H. Fang, CO_2 flux estimation by different regression methods from an alpine meadow on the Qinghai-Tibetan Plateau, in: Advances in Atmospheric Sciences, 27, Springer Science and Business Media LLC, 2010, pp. 1372–1379, https://doi.org/10.1007/s00376-010-9218-9.
[66] Senseair A.B., Delsbo, Sweden, (2025). https://senseair.com.
[67] Embenmass, MG2 datalogger (2025). http://ebenmass.it/.
[68] Bosch Sensortec GmbH (2025). https://www.bosch-sensortec.com/products/environmental-sensors/humidity-sensors-bme280.
[69] Espressif Systems, Shanghai, (2025). https://www.espressif.com/.
[70] West Systems (2017), Continuous Monitoring Flux Station, Handbook Release 3.3.
[71] R.S. Jassal, T.A. Black, Z. Nesic, D. Gaumont-Guay, Using automated non-steady-state chamber systems for making continuous long-term measurements of soil CO_2 efflux in forest ecosystems, in: Agricultural and Forest Meteorology, 161, Elsevier BV, 2012, pp. 57–65, https://doi.org/10.1016/j.agrformet.2012.03.009.
[72] N. Pirk, M. Mastepanov, F.J.W. Parmentier, M. Lund, P. Crill, T.R. Christensen, Calculations of automatic chamber flux measurements of methane and carbon dioxide using short time series of concentrations, in: Biogeosciences, 13, Copernicus GmbH, 2016, pp. 903–912, https://doi.org/10.5194/bg-13-903-2016.
[73] M. Voicu, V. Coman, N. Enache, L. Laslo, M. Matei, A. Rotaru, N. Bara, M. Boboc, S. Stanciu, G. Deak, Experimental Determination of Carbon Dioxide Flux in Soil and Correlation with Dependent Parameters, in: IOP Conference Series: Earth and Environmental Science 616, IOP Publishing, 2020 012010, https://doi.org/10.1088/1755-1315/616/1/012010. Number.
[74] D. Longo, G. Giudice, Accumulation Chamber post-processing tool, Zenodo (2025), https://doi.org/10.5281/zenodo.14790249.
[75] MathWorks®, Massachusetts – USA, (2025). https://it.mathworks.com/products/matlab.html.
[76] M.A. Fischler, R.C. Bolles, Random sample consensus, in: Communications of the ACM, 24, Association for Computing Machinery (ACM), 1981, pp. 381–395, https://doi.org/10.1145/358669.358692.
[77] P.H.S. Torr, A. Zisserman, MLESAC: a New Robust Estimator with Application to Estimating Image Geometry, in: Computer Vision and Image Understanding, 78, Elsevier BV, 2000, pp. 138–156, https://doi.org/10.1006/cviu.1999.0832.
[78] M. Camarda, S. Gurrieri, M. Valenza, Effects of soil gas permeability and recirculation flux on soil CO_2 flux measurements performed using a closed dynamic accumulation chamber, in: Chemical Geology, 265, Elsevier BV, 2009, pp. 387–393, https://doi.org/10.1016/j.chemgeo.2009.05.002.
[79] Legislative Decree 152/2006, Decreto Legislativo 3 aprile 2006, n. 152, Norme in materia ambientale (Normative Requirements on the Environment), GU n. 88 del 14 aprile, Supplemento Ordinario n (2006) 96.
[80] A. Marzo, D. Ventura, G.L. Cirelli, R. Aiello, D. Vanella, R. Rapisarda, S. Barbagallo, S. Consoli, Hydraulic reliability of a horizontal wetland for wastewater treatment in Sicily, in: Science of The Total Environment, 636, Elsevier BV, 2018, pp. 94–106, https://doi.org/10.1016/j.scitotenv.2018.04.228.
[81] D. Ventura, R. Rapisarda, L. Sciuto, M. Milani, S. Consoli, G.L. Cirelli, F. Licciardello, Application of first-order kinetic removal models on constructed wetlands under Mediterranean climatic conditions, in: Ecological Engineering, 175, Elsevier BV, 2022 106500, https://doi.org/10.1016/j.ecoleng.2021.106500.
[82] Z. Li, L. Kong, L. Hu, J. Wei, X. Zhang, W. Guo, W. Shi, Greenhouse gas emissions from constructed wetlands: a bibliometric analysis and mini-review, in: Science of The Total Environment, 906, Elsevier BV, 2024 167582, https://doi.org/10.1016/j.scitotenv.2023.167582.
[83] X. Yin, C. Jiang, S. Xu, X. Yu, X. Yin, J. Wang, M. Maihaiti, C. Wang, X. Zheng, X. Zhuang, Greenhouse Gases Emissions of Constructed Wetlands: Mechanisms and Affecting Factors, in: Water, 15, MDPI AG, 2023, p. 2871, https://doi.org/10.3390/w15162871.
[84] G. Larocca, D. Contrafatto, A. Cannata, G. Giudice, Multiparametric Monitoring System of Mt. Melbourne Volcano (Victoria Land, Antarctica), Sensors 23 (17) (2023) 7594.MDPI AG. 10.3390/s23177594.
[85] A. Cueva, T.H.M. Volkmann, J. Van Haren, P.A. Troch, L.K. Meredith, Reconciling Negative Soil CO_2 Fluxes: Insights from a Large-Scale Experimental Hillslope, in:

Soil Systems, 3, MDPI AG, 2019, p. 10, https://doi.org/10.3390/soilsystems3010010.
[86] J. Ma, Z.Y. Wang, B.A. Stevenson, X.J. Zheng, Y. Li, An inorganic CO_2 diffusion and dissolution process explains negative CO_2 fluxes in saline/alkaline soils, in: Springer Science and Business Media LLC, 3, 2013, https://doi.org/10.1038/srep02025.
[87] M. Firetto Carlino, D. Cavallaro, M. Coltelli, L. Cocchi, F. Zgur, D. Patanè, Time and space scattered volcanism of Mt. Etna driven by strike-slip tectonics, in: Scientific Reports, 9, Springer Science and Business Media LLC, 2019, https://doi.org/10.1038/s41598-019-48550-1.
[88] MAGA Mapping Gas Emission Project, (2025). http://www.magadb.net/.
[89] L. Scarfì, M. Firetto Carlino, C. Musumeci, Seismic anisotropy to investigate lithospheric-scale tectonic structures and mantle dynamics in southern Italy, in: Scientific Reports, 13, Springer Science and Business Media LLC, 2023, https://doi.org/10.1038/s41598-023-47973-1.
[90] M. Messina, M. Camarda, S. De Gregorio, R.M.R. Di Martino, V. Prano, Recent magma supply dynamic at Mt Etna volcano inferred from periodic measurements of soil CO_2 emissions, In EGU General Assembly 2023, Vienna, Austria, 24-28 Apr 2023, EGU23-16282, 10.5194/egusphere-egu23-16282.
[91] S. Guarrera, D. Vanella, S. Consoli, G. Giudice, S. Toscano, J.M. Ramírez-Cuesta, M. Milani, F. Ferlito, D. Longo, Analysis of small-scale soil CO_2 fluxes in an orange orchard under irrigation and soil conservative practices, in: Heliyon, 10, Elsevier BV, 2024 e30543, https://doi.org/10.1016/j.heliyon.2024.e30543.
[92] D. Saitta, S. Consoli, F. Ferlito, B. Torrisi, M. Allegra, G. Longo-Minnolo, J. M. Ramírez-Cuesta, D. Vanella, Adaptation of citrus orchards to deficit irrigation strategies, in: Agricultural Water Management, 247, Elsevier BV, 2021 106734, https://doi.org/10.1016/j.agwat.2020.106734.